processes

Article

Isolation, Genomic, and Proteomic Characterization of a Novel Neotropical Strain of *Bacillus thuringiensis* with Mosquitocidal Activities

Giselly Batista Alves [1], Marcelo Leite Dias [1], Eugenio Eduardo de Oliveira [2], Gil Rodrigues dos Santos [3], Bergmann Morais Ribeiro [4] and Raimundo Wagner de Souza Aguiar [1,*]

[1] Department of Biotechnology, Universidade Federal do Tocantins, Gurupi 77410-530, TO, Brazil
[2] Department of Entomology, Universidade Federal de Viçosa, Viçosa 36570-900, MG, Brazil
[3] Laboratory of Phytopathology, Universidade Federal do Tocantins, Gurupi 77410-530, TO, Brazil; gilrsan@mail.uft.edu.br
[4] Department of Cell Biology, Universidade de Brasília, Brasília 70910-900, DF, Brazil
* Correspondence: rwsa@uft.edu.br

Abstract: The combination of genomic and proteomic analyses is a useful tool for the study of novel *Bacillus thuringiensis* (*Bt*) strains, as these approaches allow the accurate identification of pesticidal proteins and virulence factors produced. Here, we isolated and evaluated the potential of a novel Neotropical *Bt* strain (TOD651) for controlling larvae of *Aedes aegypti* and *Culex quinquefasciatus* mosquitoes. Aiming for the full comprehension of the TOD651 larvicidal potential, we further evaluated the whole TOD651 genome and conducted the proteomic analysis of the TOD651 spore–crystal mixtures. Our results showed that *Bt* TOD651 similarly killed both *A. aegypti* (0.011 µg/mL) and *C. quinquefasciatus* (0.023 µg/mL) larvae, exhibiting similar potency to the commercial *Bt* strain. The genome sequence revealed that *Bt* TOD651 harbors *cry11Aa3*, *cry10Aa4*, *cry4Aa4*, *cry4Ba5*, *cyt1Aa5*, *cyt1Ca1*, *cyt2Ba13*, *mpp60Aa3*, and *mpp60Ba3*. The proteomic analysis revealed no expression of Mpp60Aa3, while all the other pesticidal proteins were expressed (Cry4Ba5 was more abundant than Cyt1Aa5). The expression of the Mppe showed the major proportions between proteases. The virulent factor neutral protease B and spore coat proteins were also expressed. The expression of relevant pesticidal proteins (e.g., Cry, Cyt, Mpp, and other pathogenic factors), whose actions can occur in a synergic relation, indicates that the biocontrol using *Bt* TOD651 may contribute to delaying the selection of resistant individuals.

Keywords: *Bacillus thuringiensis*; genome sequencing; proteomic; biorational mosquito control; pesticidal proteins

check for updates

Citation: Alves, G.B.; Dias, M.L.; Oliveira, E.E.d.; Santos, G.R.d.; Ribeiro, B.M.; Aguiar, R.W.d.S. Isolation, Genomic, and Proteomic Characterization of a Novel Neotropical Strain of *Bacillus thuringiensis* with Mosquitocidal Activities. *Processes* **2023**, *11*, 1455. https://doi.org/10.3390/pr11051455

Received: 24 February 2023
Revised: 11 April 2023
Accepted: 25 April 2023
Published: 11 May 2023

1. Introduction

The control of insect vectors of different diseases is of great importance for public health. Mosquito species such as *Aedes aegypti* (Linnaeus, 1762) (Diptera: Culicidae) and *Culex quinquefasciatus* (Say, 1823) (Diptera: Culicidae) can transmit several diseases that affect human life. For instance, *A. aegypti* can transmit yellow fever virus, dengue virus, Chikungunya virus, and Zika virus, while *C. quinquefasciatus* is capable of transmitting arboviruses such as West Nile Virus (WNV) and the *Wuchereria bancrofi* nematode, responsible for lymphatic filariasis disease [1].

The use of chemical insecticides for the control of mosquitoes, which harm the environment, has been slowly substituted around the world by biological control strategies, such as *Bacillus thuringiensis* (*Bt*) [2]. *Bt* is a Gram-positive bacterium known for its toxicity and specificity towards insect hosts due to its ability to produce and release crystal proteins (Cry and Cyt) during the sporulation stage [3]. *Bacillus thuringiensis* serovar *israelensis* (*Bti*) is one of the subspecies' most effective larvicides for mosquito control, being recommended

by the World Health Organization (WHO) [4,5]. *Bti* produces Cry and Cyt crystals (Cry4Aa, Cry4Ba, Cry10Aa, Cry11Aa, Cyt1Aa, and Cyt2Ba) that exhibit toxicity against mosquito species from the genus *Aedes*, *Anopheles*, and *Culex*, and for the black fly (Simuliidae) [4,6–8]. These proteins synergistically interact and can decrease the incidence of resistance in insect populations [4]. Some *Bti* strains can also harbor Mpp60A and Mpp60B proteins, which are present in other subspecies such as *jegathesan* and *malayensis* [8].

Improvements in the control of mosquitoes using *Bt* have involved the constant identification and characterization of novel strains and pesticidal proteins [9–12]. In addition, next-generation sequencing (NGS) has allowed the whole-genome sequencing of novel *Bt* strains and their characterization. Genome information has been important in research and applications of *Bt* because pesticidal genes are easily detected [13–15]. Furthermore, other genes related to the pathogenicity of *Bt* can be explored through this technique, such as virulence factors and other secondary metabolites [16,17].

Despite the characterization of genes coding pesticidal proteins allowing strain classification, it is the expression of these genes that determines their spectrum of activity [18,19]. In the genome sequence, not all annotated coding regions are expressed, and the genomic approach may not suffice to fully explain the toxicity differences between *Bt* strains [20,21]. For instance, many pesticidal proteins are cryptic or have insignificant levels of expression [22]. Thus, proteomic analysis of the pesticidal proteins that make up the parasporal crystal is essential to understand the toxicity of novel and commercial *Bt* strains [19]. In this context, the combination of genomic and proteomic analyses is a powerful tool for the accurate identification of pesticidal proteins and virulence factors of *Bt* strains [23–25], and estimations of the abundance of such proteins can be achieved in purified parasporal crystals and spore–crystal mixtures [25,26].

Several studies have been conducted to investigate the genomics of mosquitocidal *Bt* strains [21,27–29]. Interestingly, the proteomic analysis for pesticidal proteins responsible for mosquitocidal activities in *Bt* strains remains scarce and underexploited. Therefore, we isolated a novel *Bt* strain (*Bt* TOD651) and evaluated its insecticidal activity against larvae of *A. aegypti* and *C. quinquefasciatus*. To explore and better understand its toxicity, we sequenced the whole genome of TOD651 and performed proteomic analysis of the spore–crystal mixture.

2. Materials and Methods

2.1. Origin and Culture of Bt TOD651 Strain

The *Bt* TOD651 strain was isolated from a soil sample, collected in the state of Tocantins, Brazil (11°43′45″ S; 49°04′07″ W), according to Monnerat et al. [30]. This strain was cultured at 28 °C for 12 h in Luria–Bertani (LB) solid medium (10 gL^{-1} tryptone, 5 gL^{-1} yeast extract, 10 gL^{-1} NaCl, and 20 gL^{-1} agar). Posteriorly, a single colony of *Bt* TOD651 was transferred to an LB liquid medium and incubated (28 °C at 200 rpm for 16 h) for sporulation and DNA extraction steps. The *Bti* AM65-52 strain was isolated from a commercial sample (VectoBac®, Sumitomo, Tokyo, Japan) and used as a reference strain.

2.2. Crystal Protein Purification and SDS-PAGE Analysis

An aliquot of LB culture (3 mL) was transferred to CCY medium (30 mL) (13 mM KH2P04, 26 mM K2HP04, 0.002% (*w*/*v*) L-glutamine, 0.1% (*w*/*v*) casein hydrolysate, 0.1% (*w*/*v*) bacto casitone, 0.04% bacto yeast extract, 0.6% (*w*/*v*) glycerol, 0.05 M $ZnCl_2$, 0.5 M $MgCl_2$, 0.01 M $MnCI_2$, 0.2 M $CaCl_2$, 0.05 M $FeCl_3$) and incubated for sporulation (28 °C at 200 rpm for 72 h). Then, the spore–crystal mixture was collected, and the crystal proteins were purified according to a previously described method [31]. Purified crystals were suspended in a small volume of phosphate-buffered saline (136 mM NaCl, 1.4 mM KH_2PO_4, 2.6 mM KCl, 8 mM Na_2HPO_4, and 4.2 mL H_2O, pH 7.4), and fractionated by electrophoresis on a 10% SDS-PAGE gel [30].

2.3. Identification of Crystal Morphology

The morphological characterization of Cry protein crystals was performed by scanning electron microscopy. The spore–crystal mixture of *Bt* TOD651 was collected and diluted in sterile water. Then, a 100 µL aliquot of the diluted suspension was placed on metallic supports and dried for 24 h at 37 °C, covered with gold for 180 s using an Emitech apparatus (model K550; Quorum Technologies, Lewes, UK), and observed under a Zeiss scanning electron microscope (model DSM 962; Carl Zeiss AG, Oberkochen, Germany) at 10 or 20 Kv.

2.4. Larvae Rearing

The larvae of *A. aegypti* and *C. quinquefasciatus* were collected from fields without the application of insecticides, in regions of transition between urban and rural areas in the state of Tocantins, Brazil (11°40′55.7″ latitude S, 49°04′3.9″ longitude W). The insect colonies were established in the Entomology Laboratory of the Federal University of Tocantins, Gurupi Campus, according to Aguiar et al. [32]. The larvae were reared in plastic containers (40 cm × 25 cm × 8 cm) and fed a sterilized diet (an 80/20 mix of chick chow powder/yeast), and mosquitoes were provided with a 10% sucrose solution. We blood-fed the adult females five days after emergence with defibrinated sheep blood using a membrane feeder device [33].

2.5. Bioassays

Using the spore–crystal mixtures, bioassays were conducted on *A. aegypti* and *C. quinquefasciatus* third-instar larvae. The concentrations were determined according to Mclaughlin et al. [34]. Seven concentrations of the spore–crystal mixtures (0.05, 0.10, 0.15, 0.20, 0.25, 0.30, and 0.40 µg/mL) were tested, and sterile distilled water was used as a negative control. Bioassays were performed in 3 replicates with 25 larvae in 100 mL of distilled water. Treated larvae were kept at 26 ± 1 °C, 60.0 ± 5% RH, and a 12 h light–dark photoperiod. The number of dead and live larvae was counted after 24 h. The larvae that did not move when touched with a sterile stick were considered dead [35]. The spore–crystal mixture from the AM65-52 strain was used as a reference. Concentration–mortality curves were estimated by probity analysis using the PROBIT procedure in the SAS software [36].

2.6. Whole-Genome Sequencing, Assembly, and Annotation

Genomic DNA was extracted using the Wizard® Genomic DNA Purification Kit (Promega, Madison, WI, USA). Posteriorly, DNA concentration and purity were measured using the NanoDrop™ 8000 apparatus (Thermo Fisher Scientific, Waltham, MA, USA) and stored at −20 °C until further use. Sequencing was performed on Illumina Mi-Seq technologies, using a paired-end application, and reads with a mean length of 75.9 bp (Illumina, San Diego, CA, USA), generating a total of 15,425,426 reads with an average insert size of 200 bp and coverage of 426×. Sequence reads' quality was assessed using FastQC software version 0.11.9 [37], and reads were trimmed using the Trim and Filter tool (error probability = 0.05) of Geneious version 10.2.6 [38]. The trimmed reads were used in *de novo* assembly with the SPAdes version 3.10.0 tool and default parameters [39], and contigs ≥ 1000 bp were discarded. The CDS of contigs were predicted using RASTtk (Domain: Bacteria; Taxonomy name: *Bacillus thuringiensis*; Genetic code: 11—Archaea and Bacteria). The chromosome was assembled using contigs and reference HD-789 (NCBI Accession No. CP003763) through reference-guided *de novo* assembly [40], using the Geneious map to reference tool to assess the virulence factors of related genes. Contigs unused in the chromosome assembly were filtered and used for predicting pesticidal protein-like genes. Related genes with virulence factors were predicted using the bacterial virulence factor database (VFDB) [41]. Putative pesticidal proteins were determined using Blastx through the Btoxin_Digger tool (scaffolds as a query) [42] and a customized database (CDS predicted as a query). The customized database was created from the *Bt* pesticidal protein list available at the *Bt* nomenclature website (http://www.lifesci.sussex.ac.uk/

home/Neil_Crickmore/Bt/toxins2.html (accessed on 9 December 2022) through Geneious using the Add/Remove Database tool. CDS with homology to the *Bt* pesticidal proteins were filtered using parameters of an E-value of 0.001 and a word size of 6.

2.7. Phylogenetic Relationship

A phylogenetic tree was constructed using the *gyrB* gene (DNA gyrase subunit B), extracted from contigs sequences, and the *gyrB* genes of the *Bacillus* ssp. strains retrieved from GenBank. The alignment was performed using ClustalW, and the phylogenetic tree was created using MEGA 11 [43] from the neighbor-joining method, with 1000 replications.

2.8. LC-MS/MS Analysis

The liquid chromatography–tandem mass spectrometry (LC-MS/MS) method was used for protein detection in the spore–crystal mixture of the *Bt* TOD651 strain. The LC-MS/MS analysis was carried out at the Veritas/Life Sciences Department at the University of São Paulo (USP, Ribeirão Preto, SP, Brazil). Firstly, the spore–crystal sample was washed three times in 1× PBS (phosphate-buffered saline), resuspended in 750 µL of solubilization buffer (8 M urea, 0.5% octyl-glucopyranoside (OG), 0.05 M Tris-HCL, pH 8.8), and sonicated by 3 cycles (60 s, 30% amplitude, and shut off for 2 s) while maintained on ice. The quantification of solubilized protein was performed using the Bradford method (Protein Assay Dye Reagent Concentrate, Bio-Rad Laboratories, Hercules, CA, USA) according to the manufacturer's instructions. In the sample preparation for advanced mass spectrometry, 50 µg of the sample was subjected to disulfide bridge reduction (50 µg of DTT (Dithiothreitol), 60 min of incubation at 37 °C), followed by alkylation (250 µg of I.A (iodoacetamide), 60 min at room temperature in the dark). Following this, the sample was diluted five times in Tris-hydrochloride (0.05 M Tris-HCl, pH 8.8), and incubated using 2 µg of trypsin (Promega, V511A) at 37 °C overnight. The cleanup and desalting of the sample were performed using C18 resin (Supleco, Bellefonte, PA, USA). The column was calibrated using 2% acetonitrile containing 0.1% formic acid, and the elution was performed with 50% acetonitrile. The sample was then dried in a speed vac and applied to a mass spectrometer (Thermo Fisher Orbitrap Eclipse) coupled to a nanoflow Nano LC-MS/MS chromatography system (Dionex Ultimate 3000 RLSCnano System, Thermofisher, Waltham, MA, USA). Peptides were separated for 90 min in a nanoEase MZ peptide BEH C18 column (130 A, 1.7 µm, 75 µm × 250 mm, Waters, Milford, MA, USA) at 300 nL/min, with a 4–50% acetonitrile gradient. The data were obtained on MS1 in the range of M/Z 375–1500 (120,000 resolution, AGC target 1×10^6, maximum time of injection of 100 ms). The most abundant ions were submitted to MS/MS (30% collision energy, 1.2 m/z, AGC target 1×10^5, 15,000 resolution).

2.9. Proteomic Data Analysis

The proteomic data were processed using the PatternLabV [44]. Firstly, the customized database was created using translated CDS of the TOD651 genome through the Generate Search DB option, including a contaminant library (MS contaminant sequences, e.g., trypsin, keratins, and albumin). Then, proteomic data were analyzed against the customized database using the following parameters: The modifications selected in the search were carbamidomethyl (C), deamination (NQ), and oxidation (M). Enzyme trypsin (fully specific), two maximum missed cleavages, an initial precursor mass tolerance of 35 ppm, MS and MS/MS tolerance errors of 10 ppm, and acceptable FDR (false discovery rate) estimates of 3% at spectral, 2% at peptide, and 1% at protein levels were added as advanced parameters.

The functional annotation of the identified proteins was performed with the UniProtKB/Swiss-Prot database, and the summary graphic of functional classification was created using GO terms through the WEGO 2.0 tool (Web Gene Ontology Annotation Plot) [45].

2.10. Data Availability

The clean reads of the *Bt* TOD651 strain have been deposited at the Sequence Read Archive (SRA) under the accession number PRJNA907848.

3. Results

3.1. Protein Profile, Crystal Morphology, and Mosquitocidal Activity

The protein profile of *Bt* TOD651-purified crystals in an SDS-PAGE showed the main proteins with molecular weights of approximately 130, 70, and 27 kDa in size (Figure 1a). The ultra-structural analysis of the spore–crystal mixture indicated the presence of spherical crystals (Figure 1b).

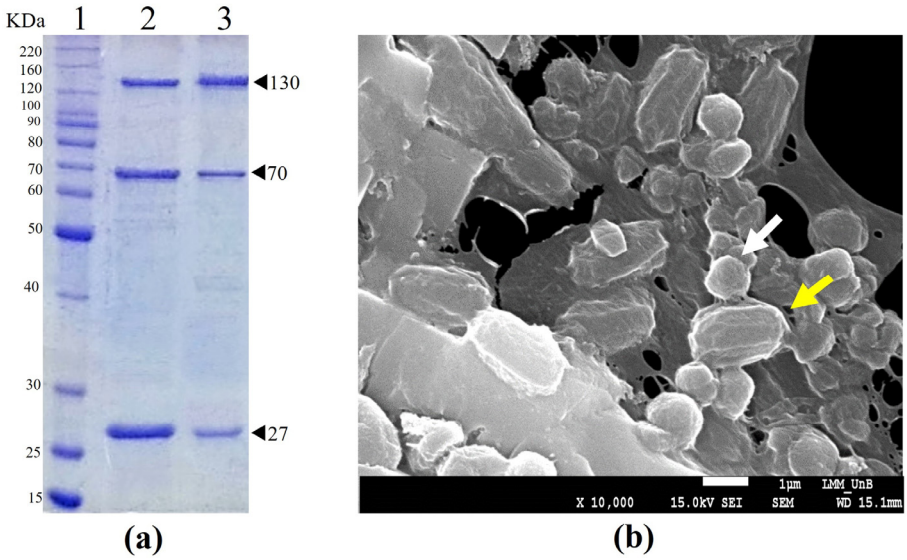

Figure 1. SDS-PAGE analysis and scanning electron microscopic image of *Bt* TOD651-purified crystals and the spore–crystal mixture. (**a**) Protein profile of *Bt* TOD651-purified crystals: Lane 1—molecular mass marker; Lane 2—AM65-52-purified crystals; Lane 3—TOD651-purified crystals. (**b**) Scanning electron micrograph of spore–crystal mixture produced by *Bt* TOD651. Arrows indicate spore (yellow) and crystal (white).

The *Bt* TOD651 spore–crystal mixture showed mosquitocidal activity towards *A. aegypti* and *C. quinquefasciatus*, with 50% lethal concentration (LC_{50}) values of 0.011 and 0.023 µg/mL, respectively (Table 1). High toxicity was observed, but the lethal concentration did not differ between the reference strain and *Bt* TOD651 for both species.

Table 1. Lethal concentration estimations of *Bt* TOD651 to larvae of *Aedes aegypti* and *Culex quinquefasciatus*.

Strain	*A. aegypti*					*C. quinquefasciatus*				
	LC_{50} (µg/mL)	**CL_{95} (µg/mL)**	**SLOPE**	**χ^2**	***p***	**LC_{50} (µg/mL)**	**LC_{95} (µg/mL)**	**SLOPE**	**χ^2**	***p***
TOD651	0.011	0.030	3.726	5.62	0.05	0.023	0.055	4.311	6.68	0.27
AM65-52	0.013	0.037	3.725	4.33	0.36	0.028	0.069	4.467	6.49	0.16

3.2. General Genomic Features

Most genes were classified into different functional classes using the RASTtk tool's analysis. The amino acids and derivatives metabolism class (579 genes), carbohydrate metabolism (320 genes), cofactors, vitamins, prosthetic groups, pigment metabolism subsystems (215 genes), protein metabolism (155 genes), cell wall and capsule (163), nucleosides and nucleotides (159 genes), and protein metabolism were the most common (Figure 2).

One hundred and eight (108) genes were grouped in the subsystem class "virulence, disease, and defense." To assess the virulence factors, the chromosome was assembled at the draft level. This sequence consisted of a chromosome with ~5.4 Mb bp containing 35.9% GC, 5130 CDS, 1 rRNA, and 71 tRNA genes (Table 2). The sequences not used in the chromosome, and presumably belonging to plasmid sequences, were used for the *cry*/*cyt* gene screening.

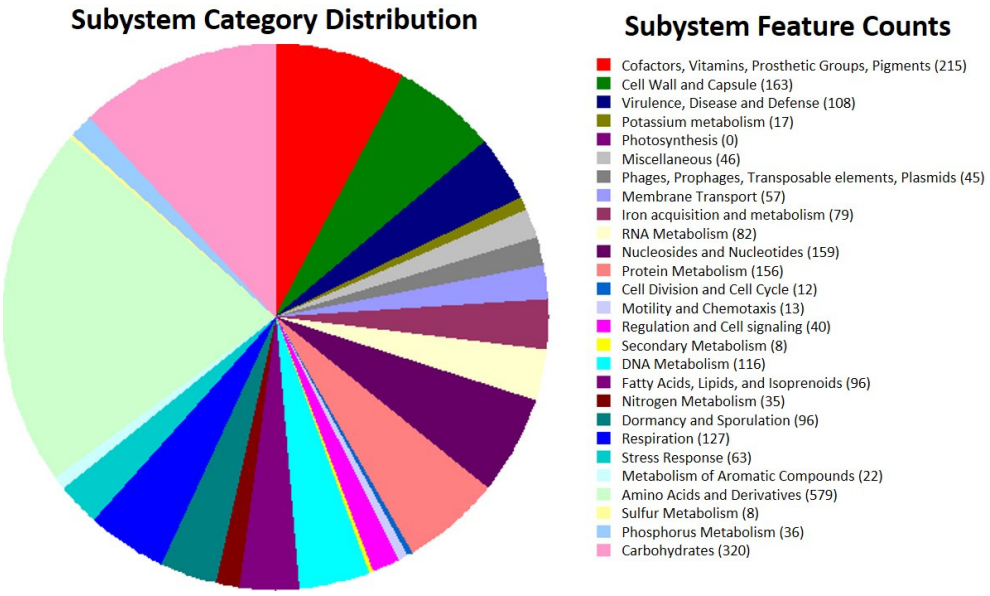

Figure 2. Subsystem category distributions in the genome of *Bt* TOD651-based functional classification.

Table 2. Draft chromosome features of the *Bt* TOD651 strain.

General Features	Value
Mean depth coverage	95.9×
Chromosome size (bp)	5,409,948
Gapped sites (%)	7.2
GC content (%)	35.9
No. of CDS	5130
No. of rRNA	1
No. of tRNA	71

3.3. Phylogenetic Analysis

Phylogenetic analysis using the *gyrB* gene showed that the *Bt* TOD651 strain formed a group closely related to three *Bti* strains (BGSC 4Q1, BGSC 4Q7rifR, and AM65-52), *Bt* MYBT18246, *Bt* ATCC 10792, and *Bt* serovar *thuringiensis* IS5056 (Figure 3).

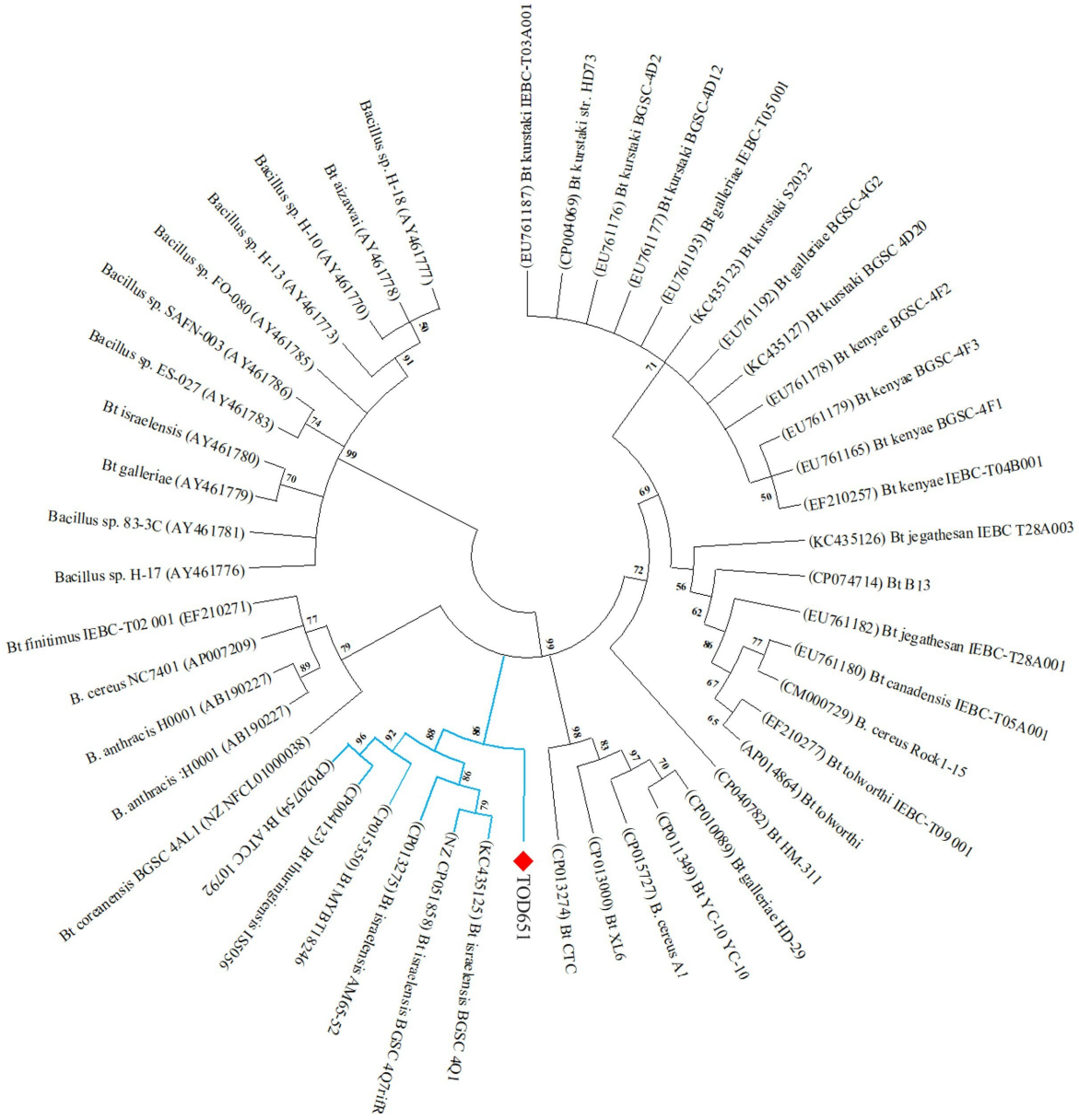

Figure 3. Phylogenetic analysis of *Bt* TOD651 with other *Bacillus* spp. based on *gyrB* sequences. The phylogenetic tree was constructed using the neighbor-joining method with 1000 bootstrap replications. Bootstrap values < 50% were disregarded for branches.

3.4. Genes Associated with Bt TOD651 Pathogenicity

Different virulence-associated genes were detected in the genome sequence (Table S1, Figure 4). Among them, enzymes (*inhA1* and *sph*), immune evasion (*bpsC* and polysaccharide capsule genes), iron acquisition genes (*dhbA-C*, *dhbE*, *dhbF*, *hal*, *ilsA*, and *asbA-F*), regulation genes (*pagR-XO2*, *papR*, *plcR*, and *cheA*), and toxins (*hlyI-III*, *hblA*, and *nheA-C*) were identified (Supplementary Table S1, Figure 4a).

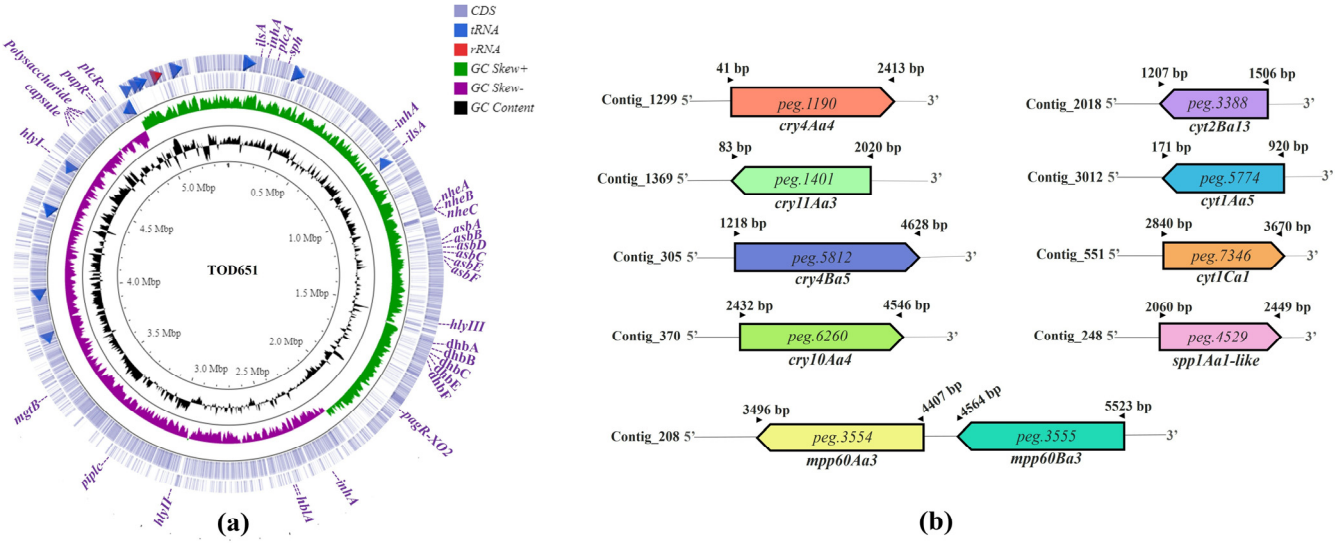

Figure 4. A graphical representation of the virulence factors and pesticidal protein-like genes found in the draft genome of *Bt* TOD651. (**a**) Distribution of virulence factor genes in the draft chromosome. (**b**) Position of pesticidal protein-like genes in contigs unused in chromosome assembly.

A total of 10 CDS predicted in the *Bt* TOD651 genome were highly homologous to pesticidal proteins (Figure 4b, Table 3). Four cry genes (*cry11Aa3*, *cry10Aa4*, *cry4Aa4*, and *cry4Ba5*), three cyt (*cyt1Aa5*, *cyt1Ca1*, and *cyt2Ba13*), two mpp (*mpp60Aa3* and *mpp60Ba3*), and one spp (*spp1Aa1*) genes were identified (Figure 4b, Table 3).

Table 3. Identification of genes coding pesticidal protein-like genes in the *Bt* TOD651.

Sequence	Predicted CDS	Length (aa)	Homologous Protein	Coverage (%)	Pairwise Identity (%)	E-Value
Contig_1299	peg.1190	698	Cry4Aa4	59.07 [1] / 99.90 [2]	99.43 [1,2]	0.0
Contig_1369	peg.1401	645	Cry11Aa3	100.00 [1,2]	100.00 [1,2]	0.0
Contig_305	peg.5812	1161	Cry4Ba5	100.00 [1,2]	100.00 [1,2]	0.0
Contig_370	peg.6260	674	Cry10Aa4	97.19 [1] / 100.00 [2]	100.00 [1,2]	0.0
Contig_2018	peg.3388	99	Cyt2Ba13	40.24 [1] / 100.00 [2]	100.00 [1,2]	0.0
Contig_3012	peg.5774	262	Cyt1Aa5	100.00 [1]	100.00 [1]	0.0
Contig_551	peg.7346	291	Cyt1Ca1	51.43 [1] / 97.80 [2]	98.90 [1,2]	0.0
Contig_208	peg.3554	323	Mpp60Aa3	100.00 [1,2]	100.00 [1,2]	0.0
Contig_208	peg.3552	319	Mpp60Ba3	100.00 [1,2]	100.00 [1,2]	0.0
Contig_248	peg.4529	323	Spp1Aa1	58.70 [1]	80.81 [1]	0.0

[1] Btoxin_Digger. [2] Customized.

3.5. Proteomics of Spore–Crystal Mixture

The detected protein sequences were functionally classified into 10 GO terms related to cellular components, 8 GO terms related to molecular functions, and 14 terms related to biological processes (Figure 5). In the cellular component groups, most proteins were mainly related to the cell part and the cell, and the molecular function classification was represented by proteins with catalytic and binding activities. Moreover, in the biological process category, the major portion of proteins belonged to metabolic and cellular processes (Figure 5).

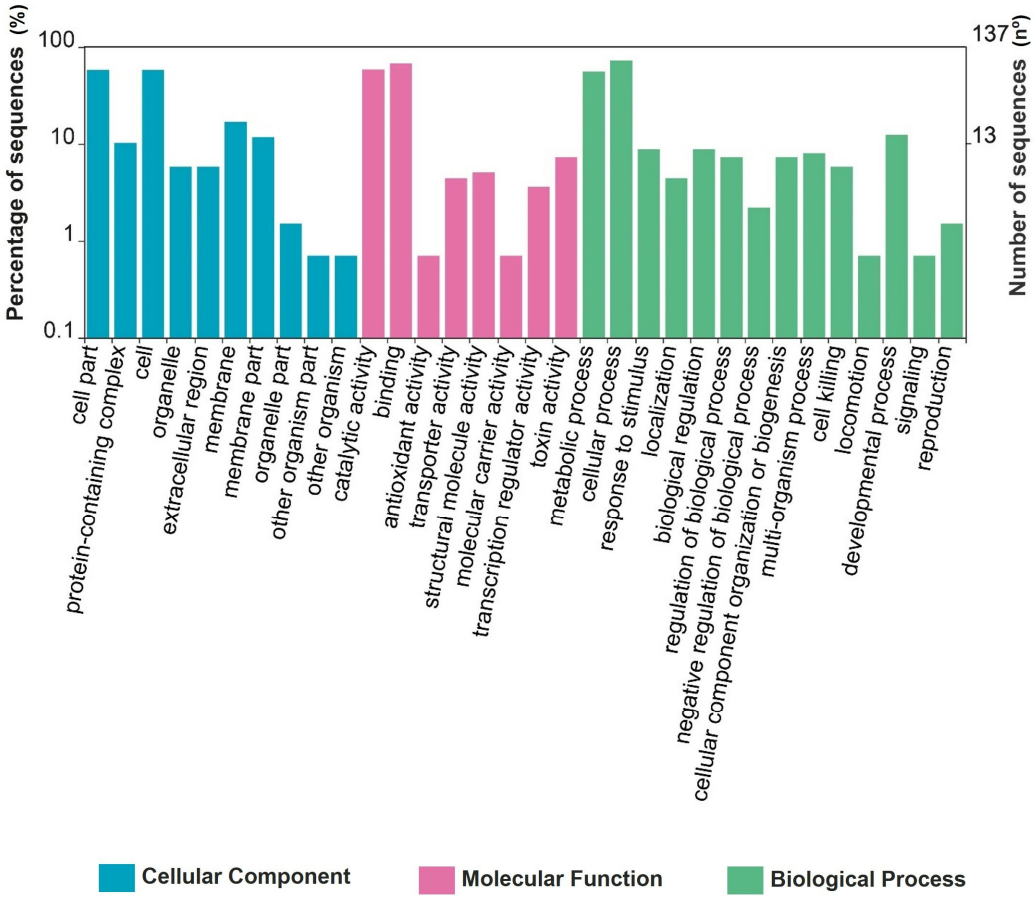

Figure 5. Functional annotation and classification of proteins identified in the spore–crystal mixture of TOD651.

A comparison of genomic and proteomic data was performed to identify the predicted CDS that were expressed. A total of 43 CDS regions annotated in the genome were detected in the proteomic analysis with at least two peptides (Table 4). With respect to pesticidal proteins, only *mpp60Aa3* did not show a unique peptide, and therefore its expression was not confirmed. Thus, the expression of Cry11Aa3, Cry10Aa4, Cry4Aa4, Cry4Ba5, Cyt1Aa5, Cyt1Ca1, Cyt2Ba13, and Mpp60Ba3 was confirmed. Cry4Ba5 was the most abundant peptide discovered (60), followed by Cry4Aa4 (47), Cry11Aa3 (46), Mpp60Aa3 (29), and Cry10Aa4 (29) (Table 4, Supplementary Table S2). Among the cytolytic proteins, Cyt1Aa was the most abundant, showing 13 unique peptides, while Cyt2Ba13 and Cyt1Ca1 showed 7 and 5 unique peptides, respectively (Table 4, Supplementary Table S2). Besides pesticidal proteins, other proteins were also identified. Metallophosphoesterase (Mppe) was the most abundant protease and showed 25 unique peptides (Table 4). Three unique peptides were from the virulence factor, extracellular neutral protease B. Proteins involved in sporulation (spore coat proteins and exosporium protein), protein biosynthesis (chaperone protein, heat-shock protein, translation elongation factor Tu, ribosomal proteins), and other functions (e.g., aminopeptidase, enolase, DNA-binding protein, RNA-binding proteins, and superoxide dismutase) were also identified (Table 4).

Table 4. Pesticidal and other proteins identified in the spore–crystal mixture of the *Bt* TOD651 strain.

CDS ID	Description [1]	Length (bp)	Peptide Sequence (No.)	Unique Peptide (No.) [4]	Coverage [5]	Protein Score [6]	NSAF [7]
peg.5812	Cry4Ba5 [2]	1136	62	60	0.5599	211.396	0.0492475
peg.1190	Cry4Aa4 [2]	791	51	47	0.6587	184.808	0.0732234
peg.1401	Cry11Aa3 [2]	645	46	46	0.6171	161.116	0.1816369
peg.3553	Mpp60Ba3 [2]	303	29	29	0.8119	97.915	0.0868883
peg.6260	Cry10Aa4 [2]	705	31	29	0.4057	104.199	0.031742
peg.3039	Metallophosphoesterase (Mppe) [3]	471	25	25	0.7113	91.843	0.0440183
peg.5774	Cyt1Aa5 [2]	249	13	13	0.6345	50.49	0.1850302
peg.1543	Heat-shock protein (GroEL)	544	9	9	0.1397	27.31	0.0060494
peg.5502	L-alanyl-gamma-D-glutamyl-L-diamino acid endopeptidase	325	9	9	0.4215	33.37	0.0131636
peg.3700	Spore coat protein (CotB)	174	8	8	0.546	28.416	0.0264785
peg.3439	Aminopeptidase	466	8	8	0.2833	27.635	0.0063558
peg.4239	Elongation factor Tu	320	8	8	0.3906	31.32	0.0133693
peg.8774	Enolase	431	7	7	0.2877	27.999	0.0068719
peg.2515	Spore coat protein (CotG)	186	7	7	0.1828	22.946	0.0212316
peg.3388	Cyt2Ba13 [2]	99	7	7	0.6768	24.895	0.0465379
peg.7343	Cyt1Ca1 [2]	85	5	5	0.2588	14.095	0.0309731
peg.7029	Dihydrolipoamide dehydrogenase of pyruvate dehydrogenase complex	470	4	4	0.0723	11.744	0.003501
peg.8531	Chaperone protein (DnaK)	611	4	4	0.0917	12.256	0.0021544
peg.5180	Spore coat protein (GerQ)	139	4	4	0.295	12.928	0.0165728
peg.5234	LSU ribosomal protein L7p/L12p(P1/P2)	119	4	4	0.5462	13.206	0.0110618
peg.7670	NAD-dependent glyceraldehyde-3-phosphate dehydrogenase	334	4	4	0.2395	16.849	0.0049265
peg.7030	Dihydrolipoamide acetyltransferase component of pyruvate dehydrogenase complex	227	4	4	0.1674	8.968	0.0072487
peg.7476	Hypothetical protein	250	3	3	0.156	10.916	0.0052654
peg.2818	Fructose-bisphosphate aldolase class II	267	3	3	0.1723	9.314	0.0049302
peg.1753	N-acetylmuramoyl-L-alanine amidase	271	3	3	0.1144	9.547	0.0048574
peg.8176	Uncharacterized protein YmfJ	82	3	3	0.4634	8.95	0.0120399
peg.4909	N-acetylmuramoyl-L-alanine amidase	327	3	3	0.1437	8.267	0.0030192
peg.3986	Extracellular neutral protease B (NprB)	426	3	3	0.1244	11.317	0.0038626
peg.9127	SSU ribosomal protein S2p (SAe)	233	2	2	0.1159	5.189	0.0028248
peg.7282	Hypotetical protein	143	2	2	0.1678	4.502	0.0046026
peg.4363	Superoxide dismutase	203	2	2	0.1823	6.977	0.0048634
peg.782	Hypothetical protein	129	2	2	0.186	5.041	0.0051022
peg.4419	Cell division trigger factor	404	2	2	0.0965	7.55	0.0016292
peg.3911	DNA-binding protein (Hbsu)	90	2	2	0.3667	7.282	0.0073131
peg.7358	Spore coat protein (CotE)	180	2	2	0.2111	6.641	0.0036565
peg.969	Phage tail fiber protein	431	2	2	0.051	4.816	0.0015271
peg.3496	Hypotetical protein	108	2	2	0.1481	4.385	0.0060942
peg.9081	Uncharacterized protein BA5373	68	2	2	0.5	6.717	0.0096791
peg.8583	RNA-binding protein (Hfq)	74	2	2	0.3243	6.323	0.0088943
peg.3589	Spore coat protein of CotY/CotZ family	155	2	2	0.2	6.649	0.0063695
peg.1544	Heat-shock protein (GroES)	94	2	2	0.2447	5.286	0.0070019
peg.5565	Tricarboxylate transport sensor protein (TctE)	92	2	2	0.3261	3.967	0.0071541
peg.8113	Exosporium protein K	118	2	2	0.1102	5.905	0.0083667

[1] Annotation based on RASTtk. [2] Classification based on Btoxin_Digger and/or the customized *Bt* database. [3] Description based on Blastx from NCBI. [4] The number of peptide sequences that are unique to the protein. [5] The percentage of the protein sequence covered by identified peptides. [6] The sum of the ion scores of all peptides that were identified. [7] Normalized spectral abundance factor: calculated using the number of spectra divided by the protein length, and then normalized over the total of spectral counts/length for all the proteins in the sample.

4. Discussion

Here, we demonstrated that a novel Neotropical *Bt* strain (TOD651), isolated from Brazilian soil samples, exhibited significant larvicidal activities against larvae of *A. aegypti* and *C. quinquefasciatus*. Such larvicidal activities were similarly potent to those recorded in *Bt* strains that are already commercialized. In addition to the characterization of *Bt* TOD651 potential to be integrated into biorational programs of mosquito control, we further explored its genome and proteome, and discovered that the pathogenicity may be derived from the expression of pesticidal proteins (e.g., Cry11Aa3, Cry10Aa4, Cry4Aa4, Cry4Ba5, Cyt1Aa5, Cyt2Ba13, and Mpp60Ba3), virulence factors (e.g., Mppe and NprB), and spore coat proteins (e.g., CoatB, CoatE, CoatG, and CotY/CotZ family proteins).

The protein profiles and ultrastructure of the parasporal crystals of the *Bt* TOD651 strain were observed to be similar to those of other anti-dipteran *Bt* strains, including the reference strain [46,47]. The SDS-PAGE 130 kDa protein band represents the Cry4 protein, the 70 kDa band indicates the presence of Cry11/Cry10, and the 27 kDa band suggests the presence of the Cyt protein [4,8]. Further, the spherical crystals observed by scanning electron microscopy showed the usual the crystal morphology found in this type of *Bt* strain [48].

The phylogenetic analysis based on the *gyrB* gene showed that *Bt* TOD651 was closely related to *Bti* strains. In addition, a nematocidal strain, *Bt* MYBT18246 [49], a type strain, *Bt* ATCC 10792 (i.e., the nomenclatural type of the species *Bt*), and a strain toxic against lepidopteran insects, *Bt* thuringiensis IS5056 [50], were also closely related to *Bt* TOD651.

The *Bt* TOD651 strain's whole-genome analysis revealed the following genes: *cry11Aa3*, *cry10Aa4*, *cry4Aa4*, *cry4Ba5*, *cyt1Aa5*, *cyt1Ca1*, *cyt2Ba13*, *mpp60Aa3*, and *mpp60Ba3*. Other genomic studies revealed a similar gene content in *Bt* strains with high mosquitocidal activity. For example, *Bt* AR23 has been described to harbor *cry10Aa4*, *cry11Aa3*, *cry4Ba5*, *cry4Aa4*, *cyt2Ba*, *cyt1Aa,* and *cyt1Ca* [28], while *Bt* LLP29 harbors *cry4Aa4*, *cry10Aa4*, *cry11Aa4*, *cyt1Aa6*, *cyt2Ba1,* and *cry22Aa* [29]. The *Bt* TOD651 genome also harbors different virulence factor genes, such as hemolysins, enterotoxins, proteases, and phospholipases. These virulence factor genes, conserved in the *Bacillus cereus* group, are responsible for the colonization and adaptation of *Bt* in insect hosts [51–53].

The proteomic analysis revealed the expression of Cry11Aa3, Cry10Aa4, Cry4Aa4, Cry4Ba5, Cyt1Aa5, Cyt2Ba13, and Mpp60Ba3 proteins. Thus, these proteins were responsible for the toxic activity of *Bt* TOD651 against *A. aegypti* and *C. quinquefasciatus*. Stein et al. [54] detected the transcripts of *cyt1Ca* but did not find Cyt1Ca protein. Here, Cyt1Ca1 protein was expressed. However, it may not be related to the toxicity of *Bt* TOD651, since neither mosquitocidal nor larvicidal activity function has been reported for Cyt1Ca [55].

Bt TOD651 showed the lower CL_{50} for *A. aegypti*. When tested individually, mosquitocidal Cry proteins have different toxicity levels between *Aedes* and *Culex* genera. The Cry4Ba protein is highly toxic against *A. aegypti*, while the Cry4Aa is highly toxic for *Culex* mosquitoes [56,57]. Cry11Aa has been linked to high toxicity against both the *Aedes* and *Culex* genera [56], whereas Cry10Aa is toxic to *A. aegypti* insects [8]. Mpp60 proteins show moderate insecticidal activity against *C. quinquefasciatus* larvae [58]. Cyt1Aa and Cyt2Ba exhibit toxicity towards both *A. aegypti* and *C. quinquefasciatus* [59,60]. However, these proteins act synergistically, which is mainly attributed to the Cyt1Aa toxin that can increase the activity of Cry4Aa, Cry4Ba, Cry11Aa, or Cry10Aa [61].

Cry10Aa has been reported as the minor protein component of *Bti* crystals [6]. In the proteomic analysis of *Bti* 4Q2-72, Cry10Aa presented a low abundance of peptides [62]. Cyt2Aa is also considered a minority pesticidal protein produced by *Bti* [63]. In the proteomic analysis of the commercial *Bti* AM65-52, Cry10Aa and Cyt2Ba were not expressed [19]. In line with the Cyt1Aa protein, the Cyt2Ba protein is also highly synergistic with the Cry proteins, and hence their combinations prevent the emergence of resistance in the target insects [4]. In addition, Cry10Aa seems to contribute to the overall toxicity of *Bti* [4]. Cry10Aa4 was one of the most abundant proteins in the spore–crystal mixture

of *Bt* TOD651, and the peptide number of Cyt2Ba13 was sufficient to not consider it as a trace-level protein.

Cyt1Aa has been reported as the major component of *Bti* AM65-52 crystals [19], while *Bti* 4Q2-72 expressed higher levels of Cry11Aa [62]. In contrast, *Bt* TOD651 expressed mainly Cry4Ba5. Cyt1Aa plays an important role in the synergism of *Bti* strains and may also contribute to delaying the evolution of resistance to Cry proteins in low proportions [64].

With respect to Mpp proteins, only Mpp60Ba3 expression was detected in this study. Even though the *mpp60Aa3* and *mpp60Ba3* genes are part of the same operon, neither of them depends on the other to be expressed [58]. SDS-PAGE gel analysis revealed no detectable protein band for Mpp60Ba3. Sauka et al. [65] discovered an *mpp* homolog in a *B. toyonensis* strain's genome but no protein bands by SDS-PAGE analysis, implying that these proteins are secreted and present in remnant fractions. The expression of Mpp60Aa and Mpp60Ba proteins has been detected in *Bti* AM65-52 [19] and *Bt jegathesan* [58] in low abundance. In contrast, Mpp60Ba3 represented a high proportion in *Bt* TOD651, suggesting that it plays an important role in the toxicity of this bacteria.

Metalloproteinases have been described as virulence factors involved in *Bt* pathogenesis, increasing the toxicity of pesticidal proteins [52]. The immune inhibitor A (InhA) has been identified as the main metalloproteinase associated with pesticidal proteins in spore–crystal mixtures of *Bt* strains [25,66]. Interestingly, in this study, the high protein homology to Metallophosphoesterase (Mppe) was the most abundant protease in *Bt* TOD651. A gene of the Mppe family has been identified in the *B. cereus* genome [67]. Mppe should play an important role in the stress resistance of bacteria to adapt to the environment/host [67]. Neutral protease B (NprB) (also named NprA and Npr99), also present in the spore–crystal mixture of *Bt* TOD651, has been associated with the virulence of *Bacillus anthracis*, degrading host tissues and increasing tissue permeability to the pathogen [68].

Other proteins that may contribute to *Bt* TOD651 toxicity were detected in the spore–crystal mixture, such as spore coat proteins. It has been demonstrated that spores in the spore–crystal mixture play a major role in *Bt* toxicity, not only due to septicemia from spore germination and outgrowth, but also due to a synergy between the spore coat protein and the crystal protein [69]. Heat-shock proteins and the elongation factor Tu were also detected, which are necessary for the formation of crystals in *Bt* strains [70,71].

The genomic and proteomic analysis of the *Bt* TOD651 and other *Bt* strains can provide insights into the genetic makeup and protein expression of the bacteria. This information can help identify the genes responsible for the bacterium's insecticidal properties, which can be used for developing new, more effective insecticides. Additionally, genomic and proteomic analyses can provide information on the evolutionary history and diversity of different *Bt* strains, which can inform their classification to aid in the development of new strains with desired traits.

The *Bt* TOD651 strain can be used as an alternative for *A. aegypti* and *C. quinquefasciatus* control, and the combined genomic and proteomic analyses revealed the proteins directly related to their toxicity. In addition, *Bt* TOD651 exhibits a variety of protein content that can potentially delay the evolution of resistance. Furthermore, we detected other proteins that can also contribute to *Bt* TOD651's pathogenicity.

Supplementary Materials: The following supporting information can be downloaded at: https://www.mdpi.com/article/10.3390/pr11051455/s1, Table S1: Virulence factors identified in the chromosome draft sequence of *Bt* TOD651 from the VFDB database. Table S2: Peptides identified for pesticidal proteins classified as unique (true) or non-unique (false).

Author Contributions: Conceptualization, all authors; methodology, G.B.A. and M.L.D.; writing—original draft preparation, G.B.A., M.L.D. and R.W.d.S.A.; writing—review and editing, B.M.R., G.R.d.S. and E.E.d.O.; supervision, R.W.d.S.A., G.R.d.S., E.E.d.O. and B.M.R.; project administration, R.W.d.S.A.; funding acquisition, R.W.d.S.A. and B.M.R. All authors have read and agreed to the published version of the manuscript.

Funding: This research was funded by the National Council of Scientific and Technological Development (CNPq—process numbers: 313455/2019-8, 427304/2018-0, 308576/2018-7), the Tocantins State Foundation for Research Aid (FAPT-SESAU/TO-DECIT/SCTIE/MS_CNPQ/No. 01/2017), and the Federal University of Tocantins (PROPESQ)—EDITAL No. 29/2020 PROPESQ, and PPGBIOTEC/UFT/GURUPI—Chamada pública para auxílio de tradução e/ou publicação de artigos cientificos—EDITAL No. 011/2020.

Data Availability Statement: All data and code generated appear in the submitted article.

Conflicts of Interest: The authors declare no conflict of interest. The funders had no role in the design of the study; in the collection, analyses, or interpretation of data; in the writing of the manuscript, or in the decision to publish the results.

References

1. Ramos-Nino, M.E.; Fitzpatrick, D.M.; Eckstrom, K.M.; Tighe, S.; Hattaway, L.M.; Hsueh, A.N.; Cheetham, S. Metagenomic analysis of *Aedes aegypti* and *Culex quinquefasciatus* mosquitoes from Grenada, West Indies. *PLoS ONE* **2020**, *15*, e0231047. [CrossRef] [PubMed]
2. Boukedi, H.; Hman, M.; Khedher, S.B.; Tounsi, S.; Abdelkefi-Mesrati, L. Promising active bioinsecticides produced by *Bacillus thuringiensis* strain BLB427. *J. Adv. Res. Rev.* **2020**, *8*, 026–035.
3. AL-FAR, I.M. *Bacillus thuringiensis* and its pesticidal crystal proteins. *Int. J. Fauna Biol.* **2020**, *3*, 157–162.
4. Ben-Dov, E. *Bacillus thuringiensis* subsp. *israelensis* and its dipteran-specific toxins. *Toxins* **2014**, *6*, 1222–1243.
5. Lutinski, J.A.; Kuczmainski, A.G.; de Quadros, S.; Busato, M.A.; Weirich, C.M.M.; Malgueiro, A.; Garcia, F.R.M. *Bacillus thuringiensis* var. *israelensis* como alternativa para o controle populacional de *Aedes aegypti* (Linnaeus, 1762) (Diptera: Culicidae). *Ciência Nat.* **2017**, *39*, 211–220.
6. Berry, C.; O'Neil, S.; Ben-Dov, E.; Jones, A.F.; Murphy, L.; Quail, M.A.; Holden, M.T.G.; Harris, D.; Zaritsky, A.; Parkhill, J. Complete sequence and organization of pBtoxis, the toxin-coding plasmid of *Bacillus thuringiensis* subsp. *Israelensis*. *Appl. Environ. Microbiol.* **2002**, *68*, 5082–5095. [CrossRef]
7. Gray, E.W.; Fusco, R. Microbial control of black flies (Diptera: Simuliidae) with *Acillus thuringiensis* subsp. *israelensis*. In *Microbial Control of Insect and Mite Pests*; Lacey, L.A., Ed.; Academic Press: Yakima, WA, USA, 2017; pp. 367–377.
8. Valtierra-de-Luis, D.; Villanueva, M.; Berry, C.; Caballero, P. Potential for *Bacillus thuringiensis* and Other Bacterial Toxins as Biological Control Agents to Combat Dipteran Pests of Medical and Agronomic Importance. *Toxins* **2020**, *12*, 773. [CrossRef]
9. Viana, J.L.; Soares-da-Silva, J.; Vieira-Neta, M.R.A.; Tadei, W.P.; Oliveira, C.D.; Abdalla, F.C.; Peixoto, C.A.; Pinheiro, V.C.S. Isolates of *Bacillus thuringiensis* from Maranhão biomes with potential insecticidal action against *Aedes aegypti* larvae (Diptera, Culicidae). *Braz. J. Biol.* **2020**, *81*, 114–124. [CrossRef]
10. Zhou, Y.; Wu, Z.; Zhang, J.; Wan, Y.; Jin, W.; Li, Y.; Fang, X. *Bacillus thuringiensis* novel toxin Epp is toxic to mosquitoes and *Prodenia litura* larvae. *Braz. J. Microbiol.* **2020**, *51*, 437–445. [CrossRef]
11. Wu, J.; Wei, L.; He, J.; Fu, K.; Li, X.; Jia, L.; Wang, R.; Zhang, W. Characterization of a novel *Bacillus thuringiensis* toxin active against *Aedes aegypti* larvae. *Acta Trop.* **2021**, *223*, 106088. [CrossRef]
12. Roy, M.; Chatterjee, S.; Dangar, T.K. Characterization and mosquitocidal potency of a *Bacillus thuringiensis* strain of rice field soil of Burdwan, West Bengal, India. *Microb. Pathog.* **2021**, *158*, 105093. [CrossRef] [PubMed]
13. Day, M.; Ibrahim, M.; Dyer, D.; Bulla, L. Genome Sequence of *Bacillus thuringiensis* subsp. *kurstaki* strain HD-1. *Genome Announc.* **2014**, *2*, e00613-14. [PubMed]
14. Jeong, H.; Choi, S.-K.; Park, S.-H. Genome Sequences of *Bacillus thuringiensis* serovar *kurstaki* strain BP865 and *B. thuringiensis*, serovar *aizawai* strain HD-133. *Genome Announc.* **2017**, *5*, e01544-16. [CrossRef] [PubMed]
15. Sajid, M.; Geng, C.; Li, M.; Wang, Y.; Liu, H.; Zheng, J.; Sun, M. Whole-genome analysis of *Bacillus thuringiensis* revealing partial genes as a source of novel *cry* toxins. *Appl. Environ. Microbiol.* **2018**, *84*, e00277-18. [CrossRef] [PubMed]
16. Lechuga, A.; Lood, C.; Salas, M.; van Noort, V.; Lavigne, R.; Redrejo-Rodríguez, M. Completed genomic sequence of *Bacillus thuringiensis* HER1410 reveals a Cry-containing chromosome, two megaplasmids, and an integrative plasmidial prophage. *G3 Genes Genom. Genet.* **2020**, *10*, 2927–2939.
17. Susič, N.; Janežič, S.; Rupnik, M.; Stare, B.G. Whole genome sequencing and comparative genomics of two nematicidal *Bacillus* strains reveals a wide range of possible virulence factors. *G3 Genes Genom. Genet.* **2020**, *10*, 881–890. [CrossRef]
18. Wu, D.; He, J.; Gong, Y.; Chen, D.; Zhu, X.; Qiu, N.; Sun, M.; Li, M.; Yu, Z. Proteomic analysis reveals the strategies of *Bacillus thuringiensis* YBT-1520 for survival under long-term heat stress. *Proteomics* **2011**, *11*, 2580–2591. [CrossRef]
19. Caballero, J.; Jiménez-Moreno, N.; Orera, I.; Williams, T.; Fernández, A.B.; Villanueva, M.; Ferré, J.; Caballero, P.; Ancín-Azpilicueta, C. Unraveling the composition of insecticidal crystal proteins in *Bacillus thuringiensis*: A proteomics approach. *Appl. Environ. Microbiol.* **2020**, *86*, e00476-20. [CrossRef] [PubMed]
20. Rang, J.; He, H.; Wang, T.; Ding, X.; Zuo, M.; Quan, M.; Sun, Y.; Yu, Z.; Hu, S.; Xia, L. Comparative analysis of genomics and proteomics in *Bacillus thuringiensis* 4.0718. *PLoS ONE* **2015**, *10*, e0119065. [CrossRef]
21. Alves, G.B.; Melo, F.L.; Oliveira, E.E.; Haddi, K.; Costa, L.; Dias, M.L.; Campos, F.S.; Pereira, E.J.G.; Côrrea, R.F.T.; Ascêncio, S.D.; et al. Comparative genomic analysis and mosquito larvicidal activity of four *Bacillus thuringiensis* subsp. *israelensis* strains. *Sci. Rep.* **2020**, *10*, 5518. [CrossRef]

22. Dankocsik, C.; Donovan, W.P.; Jany, C.S. Activation of a cryptic crystal protein gene of *Bacillus thuringiensis* subspecies *kurstaki* by gene fusion and determination of the crystal protein insecticidal specificity. *Mol. Microbiol.* **1990**, *4*, 2087–2094. [CrossRef] [PubMed]
23. Quan, M.; Xie, J.; Liu, X.; Li, Y.; Rang, J.; Zhang, T.; Zhou, F.; Xia, F.; Hu, S.; Sun, Y.; et al. Comparative analysis of genomics and proteomics in the new isolated *Bacillus thuringiensis* X022 revealed the metabolic regulation mechanism of carbon flux following Cu^{2+} treatment. *Front. Microbiol.* **2016**, *7*, 792. [CrossRef] [PubMed]
24. Gomis-Cebolla, J.; Scaramal, R.A.P.; Ferré, J. A genomic and proteomic approach to identify and quantify the expressed *Bacillus thuringiensis* proteins in the supernatant and parasporal crystal. *Toxins* **2018**, *10*, 193. [CrossRef] [PubMed]
25. Khorramnejad, A.; Gomis-Cebolla, J.; Talaei-Hassanlouei, R.; Bel, Y.; Escriche, B. Genomics and proteomics analyses revealed novel candidate pesticidal proteins in a lepidopteran-toxic *Bacillus thuringiensis* strain. *Toxins* **2020**, *12*, 673. [CrossRef]
26. Baragamaarachchi, R.Y.; Samarasekera, J.K.R.R.; Weerasena, O.V.D.S.J.; Lamour, K.; Jurat-Fuentes, J.L. Identification of a native *Bacillus thuringiensis* strain from Sri Lanka active against Dipel-resistant *Plutella xylostella*. *PeerJ* **2019**, *7*, e7535. [CrossRef]
27. Doggett, N.A.; Stubben, C.J.; Chertkov, O.; Bruce, D.C.; Detter, J.C.; Johnson, S.L.; Han, C.S. Complete genome sequence of *Bacillus thuringiensis* serovar *israelensis* strain HD-789. *Genome Announc.* **2013**, *1*, e01023-13. [CrossRef]
28. Fayad, N.; Patiño-Navarrete, R.; Kambris, Z.; Antoun, M.; Osta, M.; Chopineau, J.; Mahillon, J.; El Chamy, L.; Sanchis, V.; Awad, M.K. Characterization and whole genome sequencing of AR23, a highly toxic *Bacillus thuringiensis* strain isolated from Lebanese soil. *Curr. Microbiol.* **2019**, *76*, 1503–1511. [CrossRef]
29. Ma, W.; Chen, H.; Jiang, X.; Wang, J.; Gelbič, I.; Guan, X.; Zhang, L. Whole genome sequence analysis of the mosquitocidal *Bacillus thuringiensis* LLP29. *Arch. Microbiol.* **2020**, *202*, 1693–1700. [CrossRef]
30. Monnerat, R.G.; Batista, A.C.; de Medeiros, P.T.; Martins, E.S.; Melatti, V.M.; Praça, L.B.; Dumas, V.F.; Morinaga, C.; Demo, C.; Gomes, A.C.M.; et al. Screening of Brazilian *Bacillus thuringiensis* isolates active against *Spodoptera frugiperda*, *Plutella xylostella* and *Anticarsia gemmatalis*. *Biol. Control* **2007**, *41*, 291–295. [CrossRef]
31. Mounsef, J.R.; Salameh, D.; Kallassy, A.M.; Chamy, L.; Brandam, C.; Lteif, R. A simple method for the separation of *Bacillus thuringiensis* spores and crystals. *J. Microbiol. Methods* **2014**, *107*, 147–149. [CrossRef]
32. Aguiar, R.W.S.; dos Santos, S.F.; Morgado, F.S.; Ascencio, S.D.; Lopes, M.M.; Viana, K.F.; Didonet, J.; Ribeiro, B.M. Insecticidal and repellent activity of *Siparuna guianensis* Aubl. (Negramina) against *Aedes aegypti* and *Culex quinquefasciatus*. *PLoS ONE* **2015**, *10*, e0116765.
33. Valbon, W.; Andreazza, F.; Oliveira, E.E.; Liu, F.; Feng, B.; Hall, M.; Klimavicz, J.; Coats, J.R.; Dong, K. Bioallethrin activates specific olfactory sensory neurons and elicits spatial repellency in *Aedes aegypti*. *Pest Manag. Sci.* **2022**, *78*, 438–445. [CrossRef] [PubMed]
34. McLaughlin, R.E.; Dulmage, H.T.; Alls, R.; Couch, T.L.; Dame, D.A.; Hall, I.M.; Rose, R.I.; Versoi, P.L. US standard bioassay for the potency assessment of *Bacillus thuringiensis* serotype H-14 against mosquito larvae. *Bull. ESA* **1984**, *30*, 26–29.
35. Dulmage, H.T.; Yousten, A.A.; Singer, S.L.L.A.; Lacey, L.A. *Guidelines for Production of Bacillus thuringiensis H-14 and Bacillus sphaericus*; No. TDR/BCV/90.1; Unpublished; World Health Organization: Geneva, Switzerland, 1990.
36. SAS Institute. *SAS/STAT User's Guide*; SAS Institute: Cary, NC, USA, 2008.
37. Andrews, S. FastQC: A Quality-Control Tool for High-Throughput Sequence. 2015. Available online: https://www.bioinformatics.babraham.ac.uk/projects/fastqc (accessed on 26 October 2021).
38. Kearse, M.; Moir, R.; Wilson, A.; Stones-Havas, S.; Cheung, M.; Sturrock, S.; Buxton, S.; Cooper, A.; Markowitz, S.; Duran, C.; et al. Geneious Basic: An integrated and extendable desktop software platform for the organization and analysis of sequence data. *Bioinformatics* **2012**, *28*, 1647–1649. [CrossRef]
39. Bankevich, A.; Nurk, S.; Antipov, D.; Gurevich, A.A.; Dvorkin, M.; Kulikov, A.S.; Lesin, V.M.; Nikolenko, S.I.; Pham, S.; Prjibelski, A.D.; et al. SPAdes: A new genome assembly algorithm and its applications to single-cell sequencing. *J. Comput. Biol.* **2012**, *19*, 455–477. [CrossRef]
40. Lischer, H.E.; Shimizu, K.K. Reference-guided de novo assembly approach improves genome reconstruction for related species. *BMC Bioinform.* **2017**, *18*, 474. [CrossRef]
41. Liu, B.; Zheng, D.; Jin, Q.; Chen, L.; Yang, J. VFDB 2019: A comparative pathogenomic platform with an interactive web interface. *Nucleic Acids Res.* **2019**, *47*, D687–D692. [CrossRef]
42. Liu, H.; Zheng, J.; Bo, D.; Yu, Y.; Ye, W.; Peng, D.; Sun, M. BtToxin_Digger: A comprehensive and high-throughput pipeline for mining toxin protein genes from *Bacillus thuringiensis*. *Bioinformatics* **2021**, *38*, 250–251. [CrossRef]
43. Kumar, S.; Stecher, G.; Li, M.; Knyaz, C.; Tamura, K. MEGA X: Molecular evolutionary genetics analysis across computing platforms. *Mol. Biol. Evol.* **2018**, *35*, 1547. [CrossRef]
44. Santos, M.D.; Lima, D.B.; Fischer, J.S.; Clasen, M.A.; Kurt, L.U.; Camillo-Andrade, A.C.; Monteiro, L.C.; de Aquino, P.F.; Neves-Ferreira, A.G.C.; Valente, R.H.; et al. Simple, efficient and thorough shotgun proteomic analysis with PatternLab V. *Nat. Protoc.* **2022**, *17*, 1553–1578. [CrossRef]
45. Ye, J.; Zhang, Y.; Cui, H.; Liu, J.; Wu, Y.; Cheng, Y.; Xu, H.; Huang, X.; Li, S.; Zhou, A.; et al. WEGO 2.0: A web tool for analyzing and plotting GO annotations, 2018 update. *Nucleic Acids Res.* **2018**, *46*, W71–W75. [CrossRef] [PubMed]
46. Elleuch, J.; Jaoua, S.; Darriet, F.; Chandre, F.; Tounsi, S.; Zghal, R.Z. Cry4Ba and Cyt1Aa proteins from *Bacillus thuringiensis israelensis*: Interactions and toxicity mechanism against *Aedes aegypti*. *Toxicon* **2015**, *104*, 83–90. [CrossRef] [PubMed]
47. El-Kersh, T.A.; Ahmed, A.M.; Al-Sheikh, Y.A.; Tripet, F.; Ibrahim, M.S.; Metwalli, A.A. Isolation and characterization of native *Bacillus thuringiensis* strains from Saudi Arabia with enhanced larvicidal toxicity against the mosquito vector *Anopheles gambiae* (sl). *Parasites Vectors* **2016**, *9*, 647. [CrossRef] [PubMed]

48. Nair, K.; Al-Thani, R.; Al-Thani, D.; Al-Yafei, F.; Ahmed, T.; Jaoua, S. Diversity of *Bacillus thuringiensis* strains from Qatar as shown by crystal morphology, δ-endotoxins and *cry* gene content. *Front. Microbiol.* **2018**, *9*, 708. [CrossRef]
49. Hollensteiner, J.; Poehlein, A.; Spröer, C.; Bunk, B.; Sheppard, A.E.; Rosentstiel, P.; Schulenburg, H.; Liesegang, H. Complete genome sequence of the nematicidal *Bacillus thuringiensis* MYBT18246. *Stand. Genom. Sci.* **2017**, *12*, 48. [CrossRef]
50. Swiecicka, I.; Bideshi, D.K.; Federici, B.A. Novel isolate of *Bacillus thuringiensis* subsp. *thuringiensis* that produces a Quasicuboidal crystal of Cry1Ab21 toxic to larvae of *Trichoplusia ni*. *Appl. Environ. Microbiol.* **2008**, *74*, 923–930.
51. Vilas-Bôas, G.T.; Alvarez, R.C.; dos Santos, C.A.; Vilas-Boas, L.A. Fatores de virulência de *Bacillus thuringiensis*: O que existe além das proteínas Cry. *EntomoBrasilis* **2012**, *5*, 1–10. [CrossRef]
52. Guillemet, E.; Cadot, C.; Tran, S.L.; Guinebretiere, M.H.; Lereclus, D.; Ramarao, N. The InhA metalloproteases of *Bacillus cereus* contribute concomitantly to virulence. *J. Bacteriol.* **2010**, *192*, 286–294. [CrossRef]
53. Pohare, M.B.; Wagh, S.G.; Udayasuriyan, V. Bacillus thuringiensis as potential biocontrol agent for sustainable agriculture. In *Current Trends in Microbial Biotechnology for Sustainable Agriculture*, 1st ed.; Yadav, A.N., Singh, J., Singh, C., Yadav, N., Eds.; Springer: Singapore, 2020; pp. 439–468.
54. Stein, C.; Jones, G.W.; Chalmers, T.; Berry, C. Transcriptional analysis of the toxin-coding plasmid pBtoxis from *Bacillus thuringiensis* subsp. *israelensis*. *Appl. Environ. Microbiol.* **2006**, *72*, 1771–1776. [CrossRef]
55. Cohen, S.; Albeck, S.; Ben-Dov, E.; Cahan, R.; Firer, M.; Zaritsky, A.; Dym, O. Cyt1Aa toxin: Crystal structure reveals implications for its membrane-perforating function. *J. Mol. Biol.* **2011**, *413*, 804–814. [CrossRef]
56. Otieno-Ayayo, Z.N.; Zaritsky, A.; Wirth, M.C.; Manasherob, R.; Khasdan, V.; Cahan, R.; Ben-Dov, E. Variations in the mosquito larvicidal activities of toxins from *Bacillus thuringiensis* ssp. *israelensis*. *Environ. Microbiol.* **2008**, *10*, 2191–2199. [CrossRef] [PubMed]
57. Abdullah, M.A.F.; Alzate, O.; Mohammad, M.; McNall, R.J.; Adang, M.J.; Dean, D.H. Introduction of *Culex* toxicity into *Bacillus thuringiensis* Cry4Ba by protein engineering. *Appl. Environ. Microbiol.* **2003**, *69*, 5343–5353. [CrossRef]
58. Sun, Y.; Zhao, Q.; Xia, L.; Ding, X.; Hu, Q.; Federici, B.A.; Park, H.W. Identification and characterization of three previously undescribed crystal proteins from *Bacillus thuringiensis* subsp. *jegathesan*. *Appl. Environ. Microbiol.* **2013**, *79*, 3364–3370. [CrossRef] [PubMed]
59. Juárez-Pérez, V.; Guerchicoff, A.; Rubinstein, C.; Delecluse, A. Characterization of Cyt2Bc toxin from *Bacillus thuringiensis* subsp. *medellin*. *Appl. Environ. Microbiol.* **2002**, *68*, 1228–1231. [CrossRef]
60. Torres-Quintero, M.C.; Gómez, I.; Pacheco, S.; Sánchez, J.; Flores, H.; Osuna, J.; Mendoza, G.; Soberón, M.; Bravo, A. Engineering *Bacillus thuringiensis* Cyt1Aa toxin specificity from dipteran to lepidopteran toxicity. *Sci. Rep.* **2018**, *8*, 4989. [CrossRef]
61. Cantón, P.E.; Reyes, E.Z.; Ruiz De Escudero, I.; Bravo, A.; Soberon, M. Binding of *Bacillus thuringiensis* subsp. *israelensis* Cry4Ba to Cyt1Aa has an important role in synergism. *Peptides* **2011**, *32*, 595–600. [PubMed]
62. Fu, Z.; Sun, Y.; Xia, L.; Ding, X.; Mo, X.; Li, X.; Huang, K.; Zhang, Y. Assessment of protoxin composition of *Bacillus thuringiensis* strains by use of polyacrylamide gel block and mass spectrometry. *Appl. Environ. Microbiol.* **2008**, *79*, 875–880. [CrossRef]
63. Valtierra-de-Luis, D.; Villanueva, M.; Lai, L.; Williams, T.; Caballero, P. Potential of Cry10Aa and Cyt2Ba, two minority δ-endotoxins produced by *Bacillus thuringiensis* ser. *israelensis*, for the control of *Aedes aegypti* larvae. *Toxins* **2020**, *12*, 355.
64. Wirth, M.C.; Park, H.W.; Walton, W.E.; Federici, B.A. Cyt1A of *Bacillus thuringiensis* delays evolution of resistance to Cry11A in the mosquito *Culex quinquefasciatus*. *Appl. Environ. Microbiol.* **2005**, *71*, 185–189. [CrossRef]
65. Sauka, D.H.; Peralta, C.; Pérez, M.P.; Onco, M.I.; Fiodor, A.; Caballero, J.; Caballero, P.; Berry, C.; Del Valle, E.E.; Palma, L. *Bacillus toyonensis* biovar *thuringiensis*: A novel entomopathogen with insecticidal activity against lepidopteran and coleopteran pests. *Biol. Control* **2022**, *167*, 104838. [CrossRef]
66. Banik, A.; Chattopadhyay, A.; Ganguly, S.; Mukhopadhyay, S.K. Characterization of a tea pest specific *Bacillus thuringiensis* and identification of its toxin by MALDI-TOF mass spectrometry. *Ind. Crops Prod.* **2019**, *137*, 549–556. [CrossRef]
67. Zhang, J.; Wang, H.; Xie, T.; Huang, Q.; Xiong, X.; Liu, Q.; Wang, G. The YmdB protein regulates biofilm formation dependent on the repressor SinR in *Bacillus cereus* 0–9. *World J. Microbiol. Biotechnol.* **2020**, *36*, 165. [CrossRef]
68. Chung, M.C.; Popova, T.G.; Millis, B.A.; Mukherjee, D.V.; Zhou, W.; Liotta, L.A.; Petricoin, E.F.; Chandhoke, V.; Bailey, C.; Popov, S.G. Secreted neutral metalloproteases of *Bacillus anthracis* as candidate pathogenic factors. *J. Biol. Chem.* **2006**, *281*, 31408–31418. [CrossRef]
69. Johnson, D.E.; Oppert, B.; McGaughey, W.H. Spore coat protein synergizes *Bacillus thuringiensis* crystal toxicity for the Indianmeal moth (*Plodia interpunctella*). *Curr. Microbiol.* **1998**, *36*, 278–282. [CrossRef]
70. Ding, X.; Huang, J.; Xia, L.; Li, X.; Yuan, C.; Dan, S. A proteomic analysis approach to study insecticidal crystal proteins from different strains of *Bacillus thuringiensis*. *Biocontrol Sci. Technol.* **2009**, *19*, 289–299. [CrossRef]
71. Xie, J.; Peng, J.; Yi, Z.; Zhao, X.; Li, S.; Zhang, T.; Quan, M.; Yang, S.; Lu, J.; Zhou, P.; et al. Role of hsp20 in the Production of Spores and Insecticidal Crystal Proteins in *Bacillus thuringiensis*. *Front. Microbiol.* **2019**, *10*, 2059. [CrossRef]